Journal of Cultural Heritage 33 (2018) 100–116

Available online at
ScienceDirect
www.sciencedirect.com

Elsevier Masson France
EM|consulte
www.em-consulte.com/en

Original article

Technological and microstructural characterization of mortars and plasters from the Roman site of Qasr Azraq, in Jordan

Marta Tenconi[a,*], Ioannis Karatasios[b], Fadi Bala'awi[c], Vassilis Kilikoglou[b]

[a] Department of Archaeology, University of Sheffield, Northgate House, West Street, Sheffield, S1 4ET, United Kingdom
[b] Institute of Nanoscience and Nanotechnology, N.C.S.R. Demokritos, 153 10 Aghia Paraskevi, Athens, Greece
[c] Queen Rania's Institute of Tourism and Heritage, The Hashemite University, P.O. Box 150459, Zarqa 13115, Jordan

ARTICLE INFO

Article history:
Received 10 September 2017
Accepted 6 March 2018
Available online 28 March 2018

Keywords:
Jordan architecture
Historic mortar
Mortar characterization
SEM
XRD
Optical microscopy

ABSTRACT

This work presents the analytical results of the mortars and plasters characterization from Qasr Azraq, located in the city of Azraq (north-eastern Jordan). The castle has undergone several interventions and modifications during its service life; the archaeological surveys have shown that the actual building is a medieval reconstruction of a Roman fort, still reflecting the original structure. This research paper encompasses 64 samples from different historical periods and structures of the monument, aiming to reconstruct the timeline of different phases and to highlight technological choices. Conclusions are drawn on the basis of interpretation and integration of in situ observations, historical data and analytical data. The mortars were characterized following a multidisciplinary approach, combining macroscopic observation with petrographic examination, mineralogical analysis (XRD), microstructural and chemical analysis (SEM-EDS) and quasi-quantitative chemical analysis (pXRF) of mortar samples. Moreover, microstructural and mechanical properties of representative samples were studied. The results indicate the use of five different types of mortars, grouped based on composition and characteristics of binder and aggregates, ranging from pure lime mortars to hydraulic, gypsum-lime and earthen mortars. Overall, this paper contributes to the better understanding of building techniques and mortar production technology in the Near East during time.

1. Introduction

Qasr Azraq is a Roman castle found in the north-east of Jordan, in the major oasis of the region (Figs. 1 and 2). The main archaeological studies of the site are attributed to the extended archaeological survey conducted by Kennedy in 1982 onwards and the excavations carried out by the Department of Antiquities between 1977–2008, the best documented being the excavation directed by Ahmad Lash in 2008 [1–4]. From these previous studies, it is evident that the actual building was a Roman fort that has undergone important rebuilding and modifications.

The aim of this paper is to elucidate the technological properties of different types of mortars and plasters historically used at Qasr Azraq, to reconstruct the stratigraphy of the different phases and, when possible, to understand the dating of the different phases or interventions. Overall, the paper underlines the selective use of different raw materials for mortars production by different occupants of the castle and contributes to the wider repository of technological data on mortars and building technology of architectural monuments in the Arabic area. Moreover, this paper presents a methodological approach for grouping and studying the technological features of a large amount of mortar samples.

1.1. Historic introduction

Originally, the castle was part of the strong military presence on the defended border which characterized the eastern provinces during the Severian period and intensified under the Tetrarchy, during the 3rd century [5]. The earliest certain date for the Roman occupation of the oasis is related to Septimio Severus (193–211 AD); however, there is no evidence that directly relates the building to this period and the oldest certain date of the site is given by inscriptions found *in loco* dedicated to Diocletian and Maximilian (287–305 AD) [3]. Another inscription dedicated to Constantine provides evidence of building refurbishment during the beginning of the Byzantine period [1,6–8]. During the 5th century AD there is no evidence of occupation at Azraq, this can be the result of a period of relative peace with the Persian, as well as of a new

* Corresponding author.
E-mail address: marta.tenconi@gmail.com (M. Tenconi).

https://doi.org/10.1016/j.culher.2018.03.005
1296-2074/

Fig. 1. Aerial photography of the castle of Azraq (After APAAME [62]).

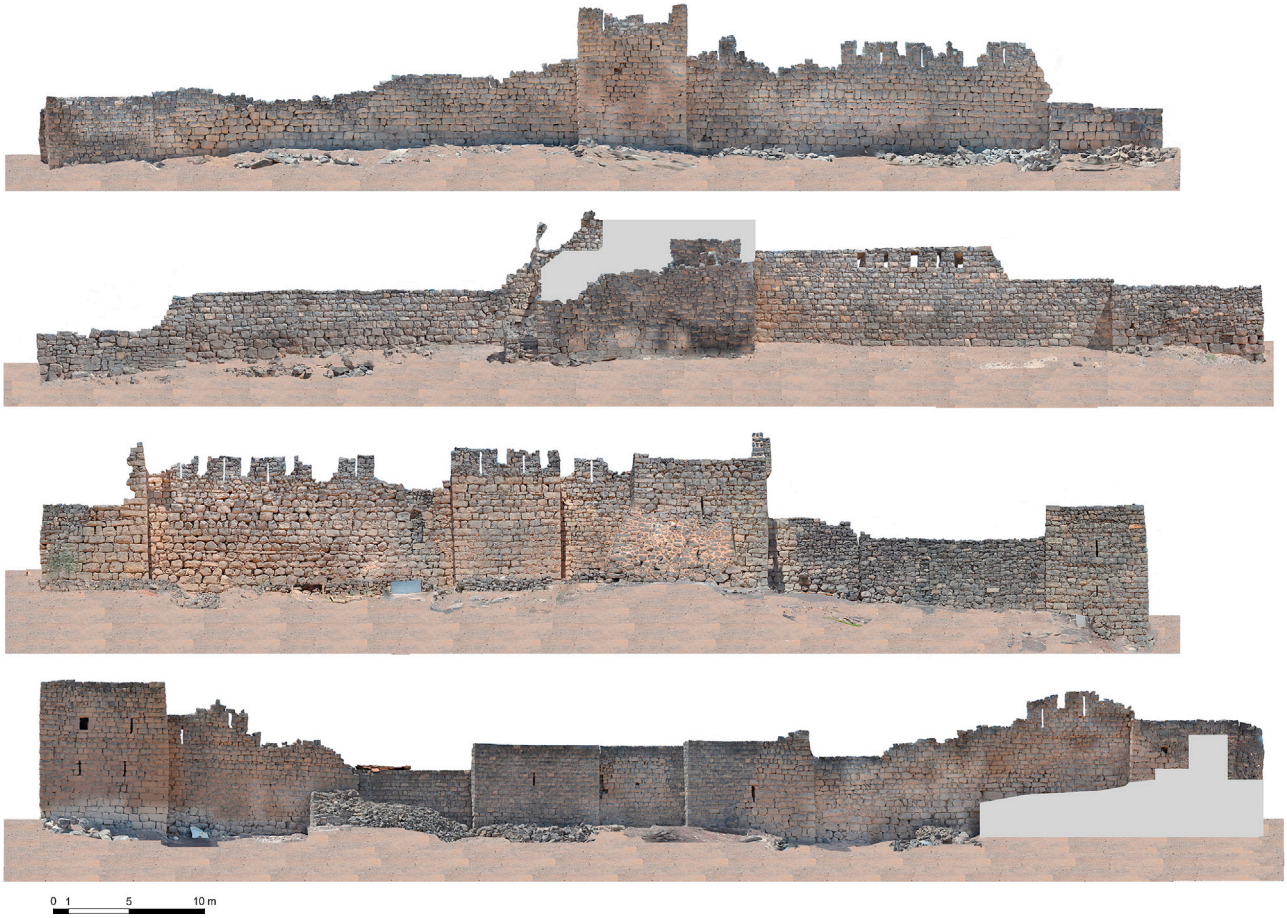

Fig. 2. Photogrammetry of the external walls of Azraq castle: a: northern external elevation; b: western external elevation; c: southern external elevation; d: eastern external elevation. Parts that it was not possible to process in grey. Photogrammetry: Marta Tenconi.

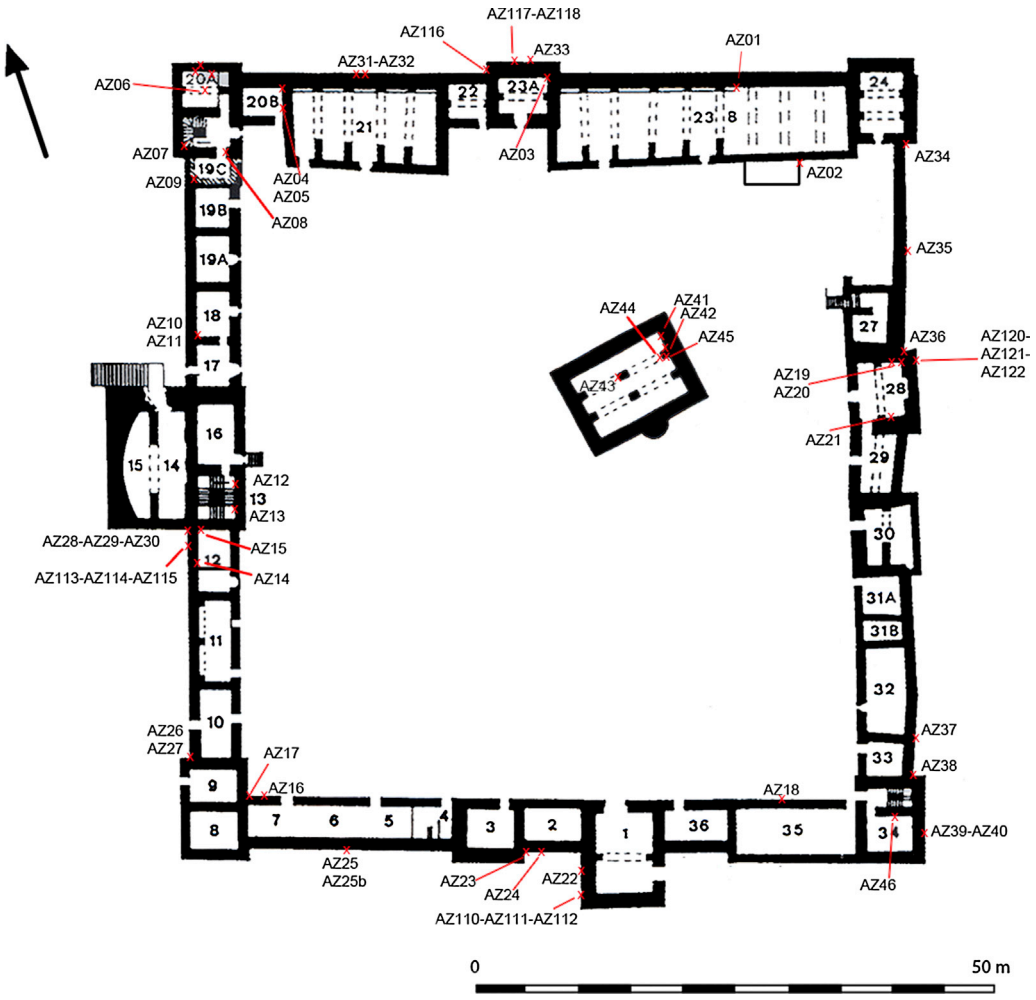

Fig. 3. Map of the castle of Azraq (after Kennedy, 2004), with sampling locations.

defensive strategy of the empire borders, employing allied nomadic Arab tribes (*Tribal Foederati*) [5,9–12]. During the early Islamic period, the fort of Azraq did not have military importance as it had in Roman and Byzantine times; its occupation is attested by the report of the Arab historian Tabari, who recorded that the Umayyad caliph Walid ibn Yazid or Walid II (709–744 AD) lived there [2–4,8,13]. Azraq acquired again military importance with the Ayyubids (1188–1263 AD), who built several new military buildings in northern and southern Jordan to secure the regions after the period of uncertainty caused by the Crusaders invasion (1100–1187 AD), still strongly present on coastal Palestine [2,3,14]. The fort maintained its importance also during the following Mamluk period (1263–1516 AD) when security on the main roads of the region was improved [14,15]. In 1516 AD, Jordan passed under the rule of the Ottoman empire (1516–1918 AD), which was a time of decline. During this time, the site was probably limited to serving as stop for the pilgrims on the road from Damascus to Mecca and Madinah [2]. The fort was used again with military purpose in 1917–1918 AD, when it became the headquarter of the Arab Army during the First War/Great Arab Revolt lead by Prince Ali bin al-Hussein and T.E. Lawrence who inhabited the south-eastern tower and the main gate tower [2,3]. Finally, between 1925 and 1930, it was inhabited by a group of Druze refugees coming from Syria since it was declared a cultural heritage site by the Department of Antiquities of Jordan (DoA), in 1953 [2,3,16]. The castle remained isolated until the end of the first half of the 20th century, when it was surrounded by the modern town [16,17].

1.2. The castle

Kennedy's surveys indicated that the castle still reflects the original structure except for a rectangular wall of boulders of nearly 100 by 125 m that originally encircled it, of which no traces survived but it is shown in a historical RAF aerial photograph dated 1922 [3,4]. The building, solely made with basalt blocks, has a square plan (79 by 72 m ca.) with large projecting square towers at the corners, and projecting towers set on the external northern, eastern and southern walls (Figs. 1–3). Internally, the rooms are located by the main walls leaving a big open courtyard in the centre. In the middle of the western wall, there is a three-story complex named *praetorium* or administrative building, which exhibits many architectural similarities with Roman forts at Qasr Bashir (Jordan), Khan Aneybeh (Syria), Avdat I (Israel) and Bourada (Numidia) [3,4,18,19]. Roofing systems used arches supporting linear corbel basalt stones on them, common in the Roman architecture of the region [20], or they used only linear corbel stones so as to support a lintelled roof. The main entrance is through the door in the southern wall of the central tower. The door is below a slightly pointed arch over which there are a machicoulis, an arrow slit, and an Arabic inscription that dates a reconstruction of the castle to the 1237 AD [2,3,14]. The actual main gate may have been made at that time and find good parallels with the coeval Ayyubid forts of Ajlun and Zarqa (Qasr Shabib) [14], it seems likely that the original entrance was on the eastern wall, between the two projecting towers, following the model of Qasr Bashir, as had been suggested by Gregory [18]. The entire castle

Fig. 4. a. Sampled mortars: a: mortar A1 (AZ33); b: mortars A1 (AZ34b) and B (AZ34); c: mortar A2 (AZ22); d: mortars A2 (AZ14b), C (AZ14c), B (AZ14b); e: mortars A2 (AZ25b) and C (AZ25); f: mortar E1 (AZ44); g–h: mortar E2 (AZ45); b: sampled mortars: a: mortar B (AZ09); b: mortar B (AZ28); c: mortar C (AZ31); d: mortar C (AZ31 covered by AZ31lw); e: mortar C (AZ26); f: mortar D1 (AZ02); g: mortar D2 (AZ03); h: mortar outlier (AZ10).

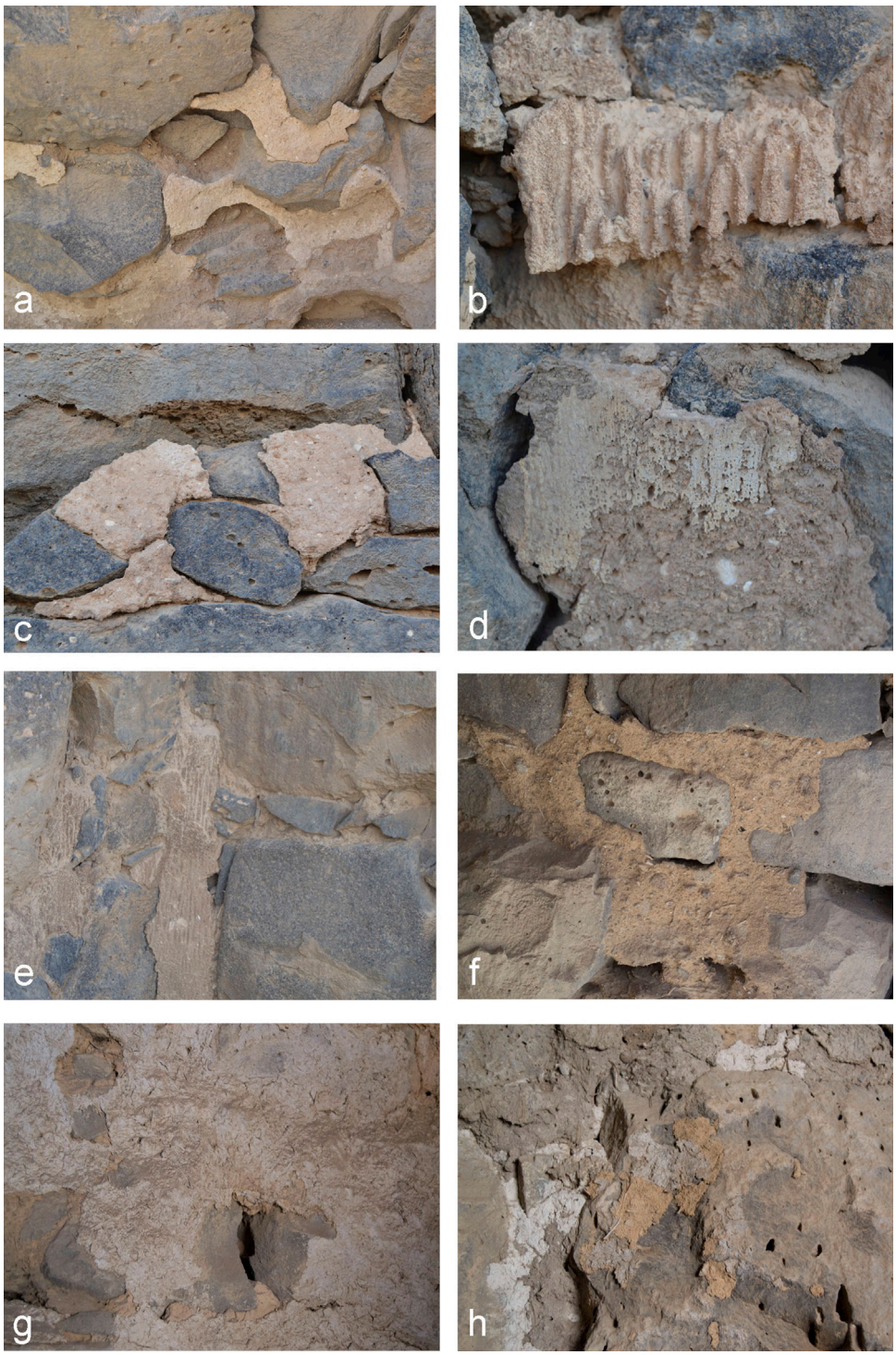

Fig. 4. *continued*

presents architectural similarities with the near Roman fort of Deir el-Kahf (Jordan) [3,4,18,19]. A small mosque of unknown date is in the courtyard.

The internal walls were initially plastered with mortars, in order to fill the gaps between basalt blocks and smooth the surface of the walls. Different types and layers of mortars have been applied during the different historical phases of the castle, which are representative of the building and construction technologies applied in different periods.

1.3. Geological background

Azraq lies in the centre of the Azraq Basin, an extensive drainage system located on the border between the north-eastern part of the Central Plateau province and the western area of the northern Basalt Plateau [21–23]. In the southern Azraq Basin Pleistocene, fluviatile-lacustrine sediments are found, primarily composed of carbonates, sandstones, shale and a flint hamada deposited on the surface, overlaying the Oligocene-Miocene sandstone and

limestone outcrops. To the east, towards the modern Saudi Arabian border, there are valleys that pass through the Cretaceous and Tertiary limestone and marl formations and form more recent deposits of a 55 m thick marly sequence of brackish to saline lacustrine deposits that contain gypsum and halite evaporites [21–23]. The Basalt Plateau that touches the northern rim of the Azraq basin, is covered by volcanic rocks mainly consisting in alkali basalt, tholeiitic basalt, basanites, hawaiites and tuffs emitted from stratovolcanos and fissure eruptions (dykes), cracked and broken in blocks by insolation weathering process and transported to the south [22,24]. The region western of Azraq, located at the northwestern margin of the Basalt Plateau, is characterized by sediments of monocrystalline quartz and calcite, less dolomite and detrital minerals as plagioclase, olivine, orthopyroxene, nepheline [25].

2. Materials and methods

According to the macroscopically recognizable characteristics of mortars, the available quantities, and their location, a sample for each type of mortar identified in different parts of the structure (external/internal walls, towers) was selected, in order to have as representative picture as possible of the site (64 samples) (Figs. 3 and 4; Table 1).

The initial grouping of the mortar samples was based on macroscopic observation and examination of freshly cut cross sections under stereomicroscope. Seventeen samples representative of all initial groups were analyzed under a petrographic microscope according to EN 12407 and UNI 11176 [26,27].

Both freshly fractured and polished cross sections of seventeen specimens were examined under a FEI Quanta Inspect D8334 scanning electron microscope (SEM) for microtextural and microchemical characterization of their matrix. Quantitative concentration of major elements was determined under SEM by energy dispersive X-ray spectrometry (EDAX PV 7760/68; standardized analysis) (SEM-EDS).

Semiquantitative concentration of major and minor elements was additionally determined on 51 mortars through X-ray fluorescence (handled Thermo Scientific Niton XL3t GOLDD+ XRF Analyzer), aiming to provide a feasibility study for the potential of portable X-ray fluorescence (pXRF) in providing an initial grouping of different types of archaeological mortars. The chemical data obtained underwent statistical analysis using Statgraphics Centurion 18 software: principal component analysis (PCA) implemented on all the samples and scatter plots of Ca vs S performed selectively on gypsum mortars.

The particle size distribution of representative mortars from each group was measured by sieve analysis in 11 samples, after mechanical separation of the binder. The mass of retained material of each sieve was weighed, after oven dried at low temperature, and the percentage of the cumulative passing material was calculated. The material with grain-size lower than 0.063 mm (binder fraction) was analyzed by X-ray powder diffraction (XRD) using a Siemens Diffrac 5000 diffractometer (Cu K-alpha = 1.541 Å, step = 0.03°/3 s) [28–30].

At least one sample from each of the main groups was selected for compressive strength determination, in an Instron 100 kN testing machine, using cubic specimens outside standard dimensions [31–33].

The hydraulicity of lime mortars was calculated through the "hydraulicity index" (HI) and the "cementation index" (CI), based on the chemical composition of the binders determined by SEM-EDS analysis:

$$CI = (2.80{*}SiO_2 + 1.1{*}Al_2O_3 + 0.7{*}Fe_2O_3)/(CaO + 1.4{*}MgO).$$

$$HI = (SiO_2 + Al_2O_3 + Fe_2O_3)/(CaO + MgO).$$

The following ranges proposed by Boynton (1980) were used as guideline for the classification of Azraq mortars: CI < 0.3, HI < 0.2, non hydraulic; CI = 0.3–0.5, HI = 0.1–0.2, feebly hydraulic; CI = 0.5–0.7, HI = 0.2–0.4, hydraulic; CI > 0.7, HI > 0.4, eminently hydraulic [34–36].

Finally, qualitative and quasi-quantitative analyses of soluble salts were carried out through colorimetric test strips (Merck MQuant) for identifying the distribution of sulphates and chlorides. For this analysis, twelve samples were collected on the four external walls, at three different heights: 10 cm, 160 cm, 290 cm.

3. Results

3.1. Mortar description

Initially, all mortar samples were macroscopically grouped giving emphasis to the color of the binder, as well as to the size, shape, type and amount of the aggregates (Figs. 4 and 5; Tables 1 and 2). In this way, five groups plus five loners were macroscopically recognized. The mineralogical and petrographic examination of these mortars by XRD, optical microscopy and SEM examination confirmed the groups previously recognised (Figs. 6 and 7; Tables 3 and 4). Mortar types A1, A2 and E1 are lime-based mortars:

- group A1 (AZ19, AZ20, AZ33, AZ34b, AZ116, AZ117, AZ118) is a heterogeneous group, however, the samples share similar morphological characteristics. They all have homogeneous micritic binder, composed by calcite (XRD), with few lumps (portions of binder not well mixed and/or partially burned limestone residual from the firing process [37,38]). Samples are crossed by big shrinkage cracks, also surrounding the aggregate (average porosity = 31%). The binder: aggregate ratio (b/a) is nearly 1/4. The aggregate is moderately sorted, mainly composed by angular to subangular fragments of micrite, sometimes under burnt, and chert (AZ19), and fewer subophitic intergranular holocrystalline basalt, very few basic porphyritic hypocrystalline volcanic rock, ultrabasic highly vesicular volcanic scoria, very rare crystals of related minerals and small quartz fragments. Both XRD and SEM-EDS show very high content of halite and rare presence of gypsum;
- group A2 (AZ01, AZ06, AZ12, AZ14b, AZ22, AZ23b, AZ25b, AZ110, AZ111, AZ112) has homogeneous, compact micritic lime binders (XRD, SEM-EDS). It has few lumps and a medium porosity (on average 34%, mainly vesicles and irregular shaped pores). The b/a ratio is nearly 1.5/1. The aggregate is characterized by moderately to well sorted, rounded fragments of volcanic scoria and hypocrystalline volcanic rock, associated with micrite (sometimes partially burned) and rare mudstone, quartz, muscovite, feldspar, olivine crystals and small basalt fragments; small charcoals are also present. Soluble salts like halite and gypsum are absent or very rare (XRD, SEM) and they were detected in higher amounts only in those samples that are renders or plasters in contact with gypsum or earthen mortars (AZ14b, AZ23b, AZ25b);
- group E1 (AZ42, AZ43, AZ44) has homogeneous micritic binder, with very small irregular shaped pores and channels (on average 40%). It differs from the other lime mortars because it has practically no aggregate (b/a = 5.5/1 ca., based on visual estimation) and consists mainly of partially burned micritic and sparitic limestone, and rare volcanic scoria, muscovite, altered mudstone, basalt fragments and related minerals. Both halite and gypsum are scarce (XRD, SEM);
- group E2 contains the only hydraulic mortar (AZ45) found at Azraq in contrast to all other lime mortars that are feebly hydraulic to not hydraulic (Table 4). It is characterized by a homogeneous, highly compact micritic binder with very low porosity

Table 1
Description of the samples with indication of mortar function, group, and color of the binder evaluated throuogh Munsell soil color chart [50].

Sample	Mortar function	Group	Binder color
AZ01	Pointing	A2	White
AZ02	Pointing	D1	Light yellowish brown
AZ03	Plaster	D2	White
AZ04	Plaster	D2	White
AZ05	Pointing	D1	Very pale brown
AZ06	Pointing	A2	White
AZ07	Plaster covering earthen mortar	C	Very pale brown
AZ08	Paving mortar	B	Light grey
AZ09	Plaster	B	Light grey
AZ10	Plaster	Outlier	White
AZ11	Plaster	B	Light grey
AZ12	Pointing/plaster, smoothed surface	A2	White
AZ13	(Too small)	Outlier	White
AZ14	Pointing?, Rough surface	C	Very pale brown
AZ14b	Plaster, smooth surface	A2	White
AZ14c	Plaster, rough surface	B	Light grey
AZ15	Structural	C	Pale yellow
AZ16	Pointing	Outlier	Very pale brown
AZ16b	Pointing	Outlier	Very pale brown
AZ17	Pointing	Outlier	Pale yellow
AZ18	Render? Covering the earth between the stones	C	Pale yellow
AZ19	Plaster covering the earth between the stones	A1	White
AZ20	Plaster covering the earth between the stones	A1	White
AZ21	Too small, pointing?	C	Pale yellow
AZ22	Pointing	A2	White
AZ23	Pointing	D2	Light grey
AZ23b	Render	A2	White
AZ24	Render	B	Very pale brown
AZ25	Pointing	C	Pale yellow
AZ25lw	Lime wash		Very pale brown
AZ25b	Render, smooth	A2	Very pale brown
AZ26	Pointing, vermiculated	C	Pale yellow
AZ27	Pointing, vermiculated	C	Pale yellow
AZ28	Pointing, vermiculated	C	Very pale brown
AZ29	Pointing, vermiculated	B	Light grey
AZ30	Pointing	C	Very pale brown
AZ31	Pointing	C	Very pale brown
AZ31lw	Lime wash		White
AZ32	Salt crystals		Light brownish grey
AZ33	Pointing, smoothed	A1	White
AZ34	Pointing, vermiculated	B	Very pale brown
AZ34b	Pointing	A1	White
AZ35	Salt concentration	D1	Greyish brown
AZ36	Pointing, vermiculated	B	Light grey
AZ37	Pointing (vermiculated?)	C	Very pale brown
AZ38	Pointing, vermiculated	B	Light grey
AZ39	Pointing	B	Light grey
AZ40	Pointing	B	Light grey
AZ41	Pointing	D2	White
AZ42	Plaster	E1	Very pale brown
AZ43	Plaster	E1	Very pale brown
AZ44	Plaster	E1	Very pale brown
AZ45	Pointing	E2	Very pale brown
AZ110	Pointing	A2	White
AZ111	Pointing	A2	White
AZ112	Pointing	A2	White
AZ113	Pointing	B	Light grey
AZ114	Pointing	B	Light grey
AZ115	Pointing	B	Light grey
AZ116	Pointing	A1	White
AZ117	Pointing	A1	White
AZ118	Pointing	A1	White
AZ120	Pointing	C	Very pale brown
AZ121	Pointing	C	Very pale brown
AZ122	Pointing	C	Very pale brown

Mortar functions: plaster mortar coats the internal wall' surfaces for decoration and protection; render mortar coats the external wall' surfaces to protect the covering structures of the building; pointing mortar lies between the stones acting as a bedding and varies from fine joints in the ashlar stonework to larger joints in the rubble masonry walls, on the external walls sometimes it partially coated the basalt stones as a render, too.

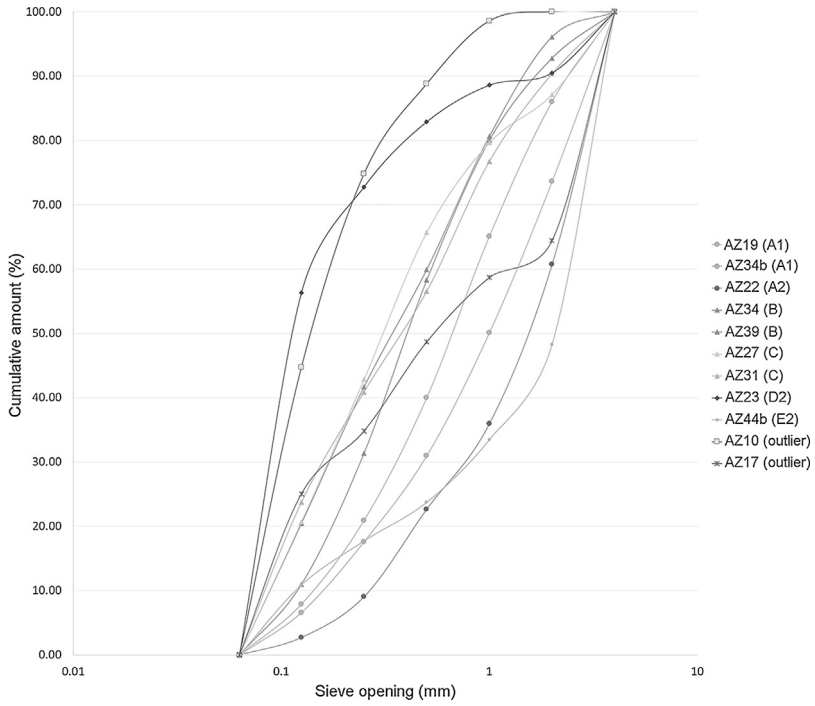

Fig. 5. Cumulative grain-size distribution curves of the aggregate fraction greater than 63 μm.

(vesicles and reaction pores surrounding the aggregate). SEM-EDS data on the binder matrix indicate Ca as the main constituent with low amounts of Si (12–26%), Al (3–7%) and K (1.8–2.6%), while XRD analysis detected calcium aluminium hydroxide carbonate hydrate phases and quartz. The b/a ratio is nearly 1/2.4 by volume. The aggregate is moderately sorted and almost exclusively represented by angular fragments of partially burned micritic and sparitic limestone, associated with few calcite crystals, mudstone and very rare basalt fragments, altered plagioclase and altered ferromagnesium minerals. Halite and gypsum are present in very small amount (XRD, SEM). Based on SEM-EDS results, the hydraulic character of AZ45 is attributed to the presence of active clay-based aluminosilicate phases (mainly due to the high Si, Al and K concentrations) in the binder fraction, leading to the reaction between lime and fine aluminosilicate particles. The result was the formation of the hydraulic phases that have been determined both on the microstructure of the binder matrix during SEM examination of the fractured sections (Fig. 7g-h) and by XRD.

Mortars of groups B and C were produced by mixing a sulphate binder with lime in similar amount, as shown by SEM-EDS chemical analysis:

- group B (AZ08, AZ09, AZ11, AZ14c, AZ24, AZ29, AZ34, AZ36, AZ38, AZ39, AZ40) is a heterogeneous group, with micritic to microsparitic binders, with areas in which sulphate and lime are in similar proportion and others where one of these minerals is predominant. Ca/S ratio (SEM-EDS) is comprised between 0.8 and 2. XRD data show also few anhydrite and rare clay minerals like smectites and kaolinite. The aggregate is abundant (b/a ratio nearly 1/1) and very poorly sorted, it is composed by rounded-subrounded fragments of micrite, sometimes partially burned, and fibrous interlocking crystals of gypsum, associated with less basalt, very rare mudstone, crystals of olivine, pyroxene, feldspars and muscovite. Sample AZ14c contains also abundant hypocrystalline volcanic rock and volcanic scoria fragments, and rare polycrystalline quartz. Sample AZ24 is highly altered. Mortars of type B have big vesicles and pores (average porosity = 26%). Halite was always detected in moderate amount (XRD, SEM) and it is abundant only in sample AZ34, which contains also small amount of the evaporite georgeite ($K_2Ca_5(SO_4)_6{\cdot}H_2O$) [39];
- group C (AZ07, AZ14, AZ15, AZ18, AZ21, AZ25, AZ26, AZ27, AZ28, AZ30, AZ31, AZ37, AZ113, AZ114, AZ115, AZ120, AZ121, AZ122) is very homogeneous, with b/a ratio of 2.4/1 and a low poros-

Table 2
Open porosity (%) and apparent density (ρa) of the analyzed mortars, determined by hydrostatic weighting [63].

Sample	ρa	% porosity
AZ07	1576.8	24.2
AZ08	1519.9	24.0
AZ09	1411.8	30.3
AZ11	1567.1	24.4
AZ12	1524.7	34.0
AZ14b	1413.0	28.9
AZ15	1287.7	32.9
AZ18	1757.8	12.8
AZ19	1697.8	35.9
AZ20	1903.8	23.9
AZ21	1633.3	20.9
AZ22	1284.5	47.9
AZ24	1429.3	33.8
AZ25b	1419.3	24.0
AZ26	1425.3	25.5
AZ27	1621.7	17.0
AZ28	1321.6	28.5
AZ29	1467.8	26.6
AZ30	1335.4	31.9
AZ31	1375.9	26.0
AZ33	1647.1	33.5
AZ34b	1511.5	31.9
AZ36	1323.2	34.6
AZ37	1443.9	27.0
AZ38	1602.7	19.4
AZ39	1427.0	25.2
AZ40	1626.4	18.9
AZ40	1626.4	18.9
AZ43	1364.0	44.2
AZ44	1375.2	43.4

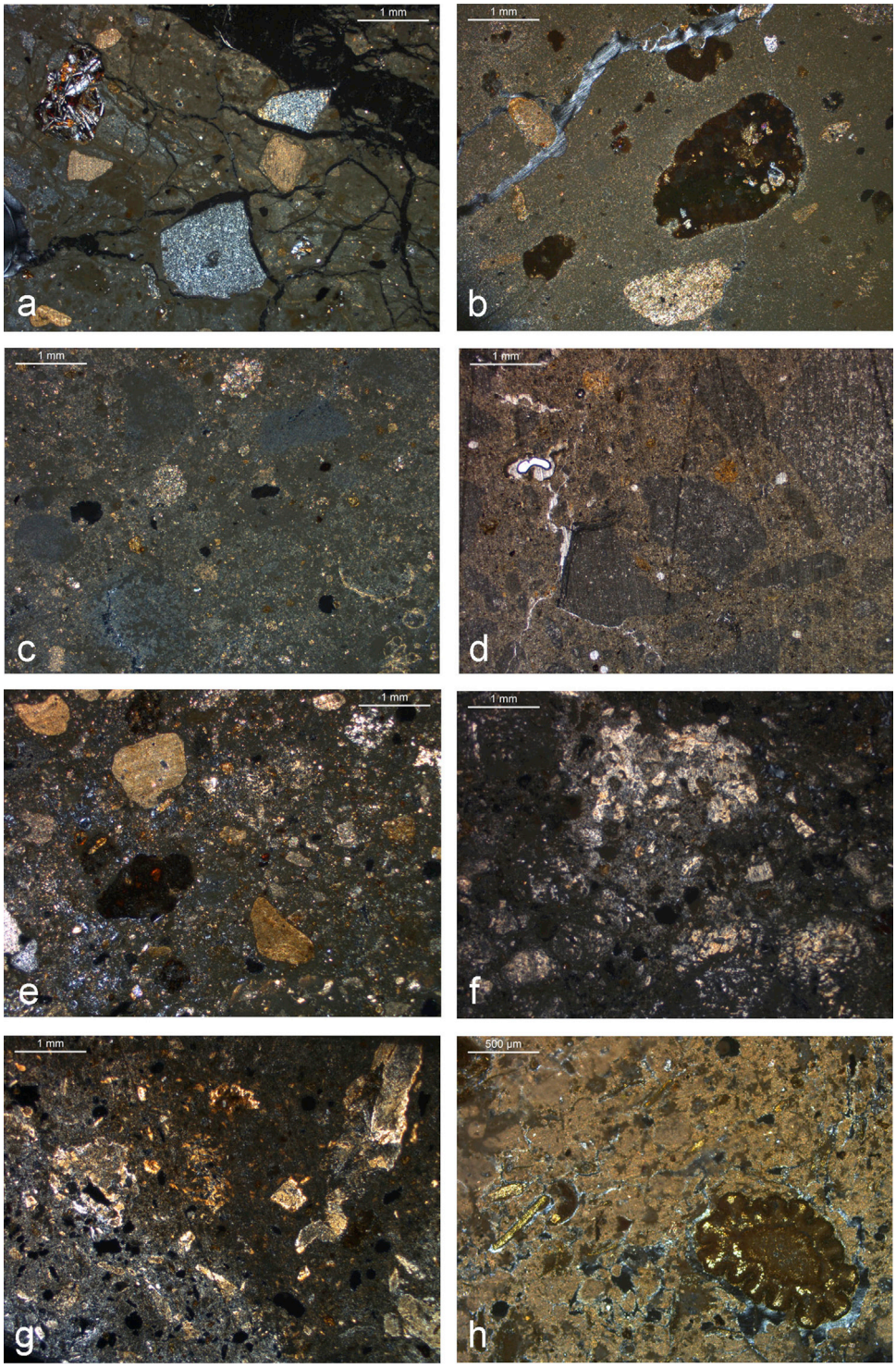

Fig. 6. Thin section photomicrographs of selected mortars analyzed in this study: a: mortar A1 (AZ19); b: mortar A2 (AZ06); c: mortar E1 (AZ44); d: mortar E2 (AZ45); e: mortar B (AZ14); f: mortar B (AZ34); g: mortar C (AZ18); h: mortar D2 (AZ23). Images a–c and e–h taken in crossed polars, image d taken in plane polars.

ity (25%, irregular shaped pores and vesicles). Gypsum is more abundant than calcite (Ca/S ratio between 0.7 and 1.4, SEM-EDS). The aggregate is predominantly composed by big fibrous interlocking crystals of gypsum, fewer limestone and calcite crystals; rare fragments of basalt and related minerals are also present, together with rare quartz and smectites. Anhydrite is always present in small amount and halite is absent or present in very small amount (XRD);

- group D is composed of earthen mortars. It is a heterogeneous group that can be subgrouped based on the binder color: brown in subgroup D1 (AZ02, AZ05, AZ35) and white to pale grey in D2 (AZ03, AZ04, AZ23, AZ41). Pointing mortar AZ23 and plaster AZ04 were chosen for the analysis: plaster AZ04 is characterized

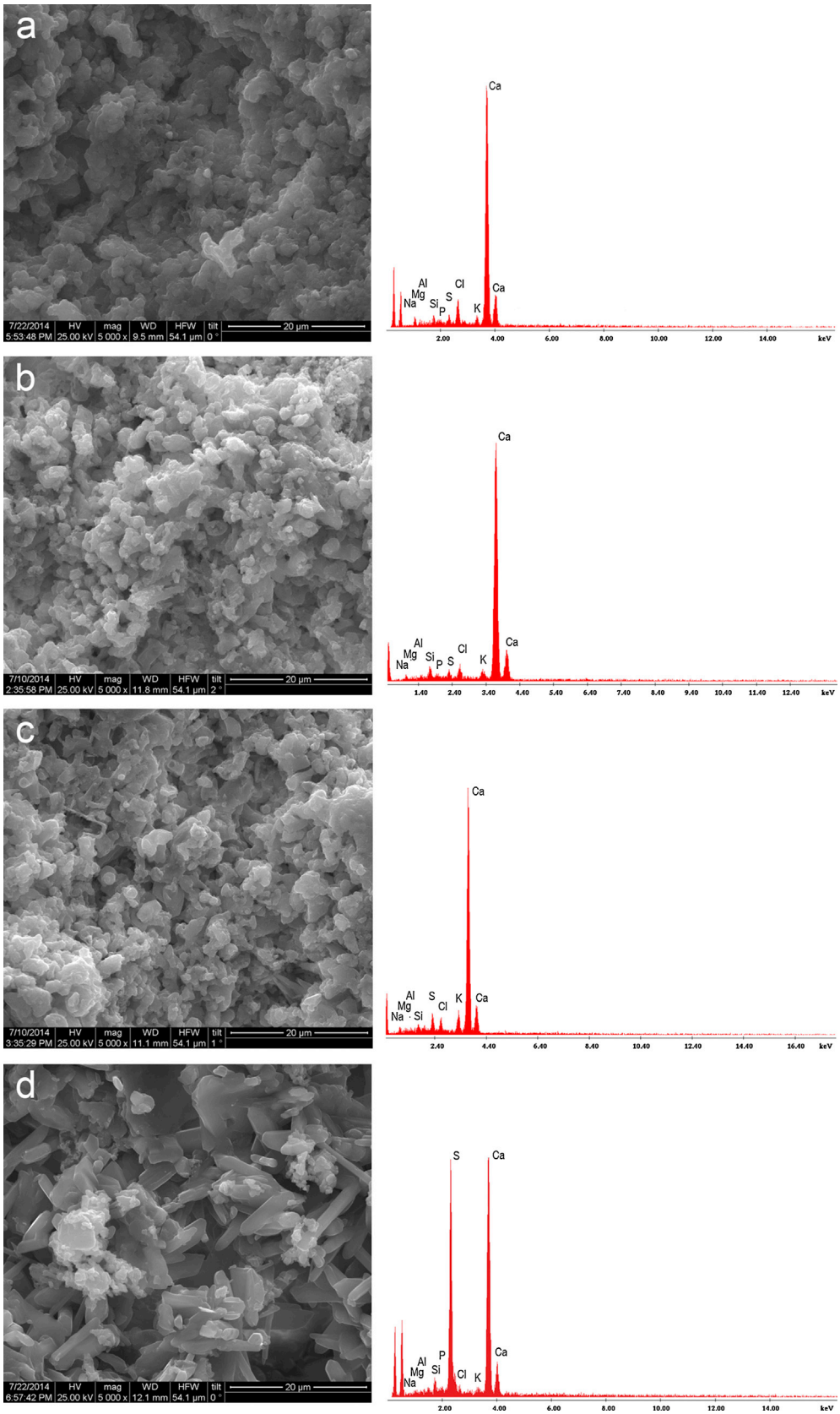

Fig. 7. BSE–SEM images showing the different microtextures that characterize the mortar binders and related SEM-EDS spectra: a: mortar A1 (AZ34b); b: mortar A2 (AZ14b); c: mortar E1 (AZ44); d: mortar B (AZ39); e: mortar C (AZ31); f: outlier AZ17; g–h: mortar E2 (AZ45); i: outlier AZ10.

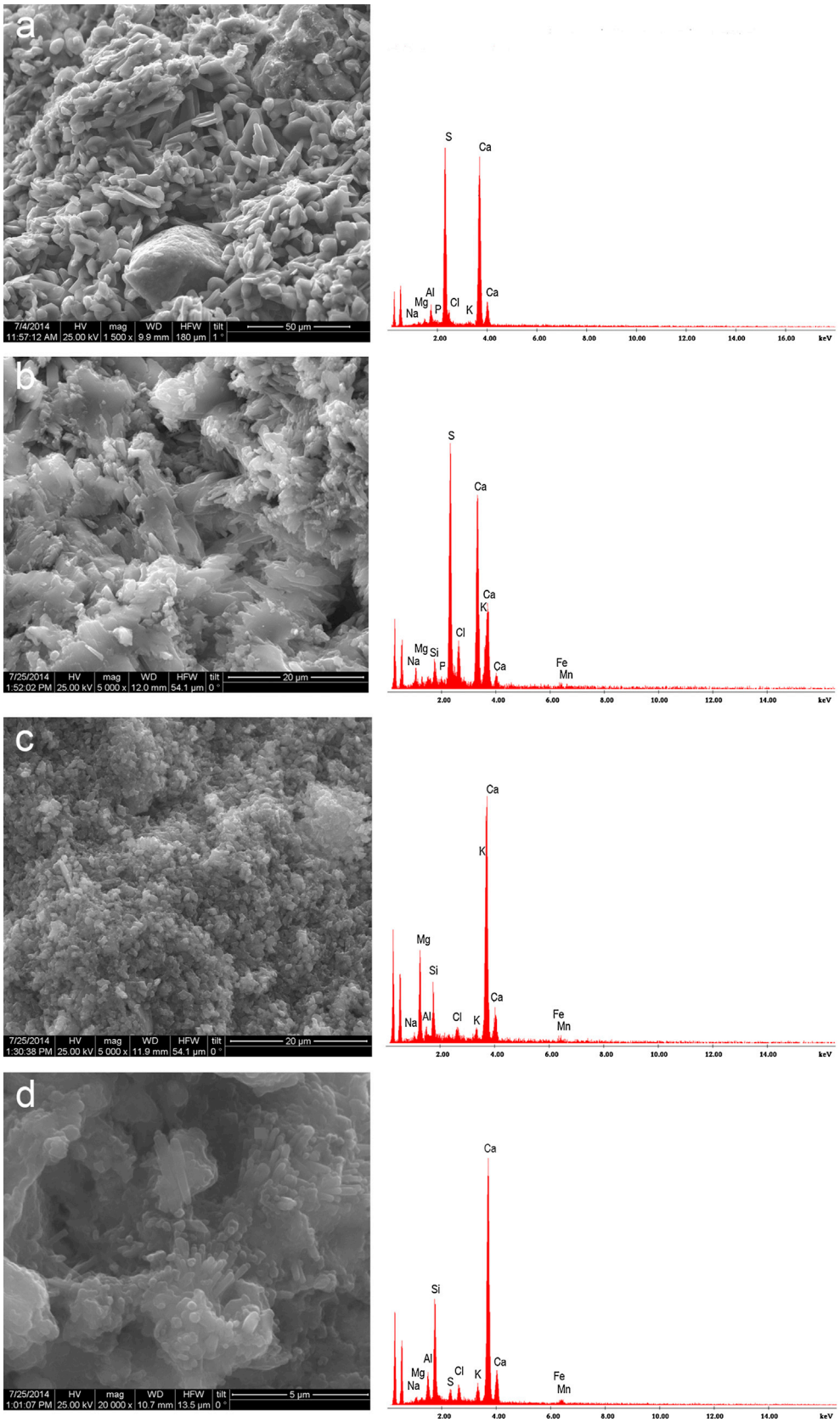

Fig. 7. *continued*

Table 3
Mineralogical associations detected in the studied mortars by XRD.

Samples	Mortar type	Gp	Cal-MCal	Dol	Brc	Qz	Hl	Anh	Ilt-Mnt	Kln	Syn	Grg	Pl	AFm
AZ19	A1	[d]?	[b]			[d]	[a]				[c]			
AZ34b	A1	[d]	[b]			[d]	[a]							
AZ22	A2		[a]			[d]							[d]	
AZ34	B	[b]	[b]			[d]	[a]	[c]		[d]		[c]		
AZ39	B	[a]	[a]			[d]	[c]	[c]	[d]	[d]				
AZ27	C	[a]	[b]			[c]	[c]	[d]	[d]					
AZ31	C	[a]	[b]			[c]		[d]	[d]					
AZ23	D2	[d]	[b]	[c]		[c]	[c]	[d]?	[d]	[d]?			[d]	
AZ45	E2	[d]	[a]		[d]?	[d]	[d]						[d]	[d]
AZ10	Outlier	[d]	[c]	[a]	[d]?	[c]	[c]		[d]	[d]			[d]	
AZ17	Outlier	[d]	[d]			[c]	[c]	[d]?		[d]	[a]			

Gp: gypsum, Cal: calcite, Mcal: magnesian calcite, Dol: dolomite, Brc: brucite, Qz: quartz, Hl: halite, Anh: anhydrite, Ilt-Mnt: illite-montmonillonite, Kln: kaolinite, Syn: syngenite, Grg: georgeite, Pl: plagioclase, AFm: calcium aluminum hydroxide carbonate hydrate.

[a] Very abundant.
[b] Abundant.
[c] Common.
[d] Scarce.

Table 4
Hydraulicity index (HI) and cementation index (CI) of the lime mortars, calculated on the SEM-EDS data.

Sample	Mortar type	MgO	Al2O3	SiO2	CaO	Fe_2O_3	HI	CI
AZ22_01	A2	1.79	1.61	3.33	75.49	0.44	0.07	0.15
AZ23b_01	A2	5.17	2.05	6.74	44.31	0.53	0.19	0.42
AZ23b_02	A2	7.72	3.41	9.74	64.69	1.61	0.20	0.43
AZ25b_01	A2	1.91	1.92	3.44	79.29	0.31	0.07	0.15
AZ25b_02	A2	1.34	2.23	2.78	83.15	0.00	0.06	0.12
AZ25b_03	A2	2.26	2.12	2.43	80.53	1.10	0.07	0.12
AZ25lw	A2	1.80	1.71	6.26	55.63	0.75	0.15	0.34
AZ34b_01	A1	1.46	1.04	2.11	44.13	0.78	0.09	0.16
AZ34b_02	A1	1.83	1.89	4.49	62.85	1.18	0.12	0.24
AZ34b_03	A1	1.94	1.78	3.19	28.02	0.90	0.20	0.37
AZ44_01	E1	1.64	1.28	3.11	72.54	1.96	0.09	0.15
AZ44_02	E1	2.97	2.23	4.64	67.64	1.87	0.12	0.23
AZ44_03	E1	0.70	1.16	2.51	51.31	1.51	0.10	0.18
AZ44_04	E1	2.37	4.35	12.61	62.19	3.17	**0.31**	**0.65**
AZ45_01	E2	1.54	2.99	11.74	72.65	0.62	0.21	0.49
AZ45_02	E2	2.07	7.23	27.71	48.09	2.31	**0.74**	**1.71**
AZ45_03	E2	1.78	7.40	25.84	47.07	2.11	**0.72**	**1.65**
AZ45_04	E2	3.15	4.42	13.24	59.20	1.76	**0.31**	**0.68**

Values indicative of hydraulic and eminently hydraulic mortars are bold.

by a micritic binder with very few aggregate and very low porosity, irregular shaped voids and channels. The aggregate is very poorly sorted, predominantly composed by big round limestone and mudstone fragments, and less basalt, quartz, plagioclase feldspars, and mica; plant fibres are also present in very small amount. Sample AZ23 is characterized by a very high porosity and few aggregate (b/a = 2.4/1). The binder has a micritic texture and it is mainly composed of magnesian calcite and dolomite, mixed with few smectites and kaolinite (XRD). Halite is present in moderate amount. The aggregate is very poorly sorted, mostly represented by round micritic limestone, dolomite, plant fibres, muscovite, basalt and related minerals.

Finally, samples AZ10, AZ13, AZ16, AZ16b, AZ17 and AZ32 were classified as outliers since they differ from any other mortar found at the site. Of these, only samples AZ10 and AZ17 were selected for the analyses: sample AZ10 is characterized by a fine binder with very few aggregate (b/a = 7.4/1). XRD and SEM-EDS analyses of the binder revealed a predominant presence of dolomite, together with some calcite. The aggregate is represented by rare very small quartz, smectites and kaolinite particles. Gypsum is present in small amount, while halite is abundant (XRD). Sample AZ17 is characterized by a fine binder with few aggregate (b/a = 1.8/1); both XRD and SEM-EDS analysis revealed the predominant presence of syngenite, together with gypsum. There are also halite and smaller amount of quartz, calcite and kaolinite. Samples AZ10 and AZ17 were not analyzed by optical microscopy.

The above groups were also confirmed by chemical analysis (Fig. 8; Table 5). The score plot of the PCA shows a similar situation (Fig. 8a): samples belonging to mortar type A1 are highly affected by their high content of halite and are concentrated towards the direction of Cl. Samples of groups A2, E1 and E2 (lime mortars) are concentrated towards high value of Ca. Only a few samples are concentrated towards lower principal component 2 (AZ01, AZ06, AZ12), and principal components 1 and 2 (AZ43, AZ44), probably because affected by small contents of halite and gypsum, respectively. Samples of mortars B and C, prepared with a mixture of gypsum and lime, are concentrated towards the direction of S, and separated because of the common presence of Cl in mortar C. Mortar D1 does not show any specific trend, and its samples are concentrated towards high values of principal component 1, where Al, Si, Fe, Mn are strong. Mortars D2, except sample AZ04, are well grouped and concentrated at low values of both principal components 1 and 2, probably because of lower content of clay minerals, due to the lime mixing, and to the presence of some halite. Finally, outliers are spread in the graph from lower (AZ10, AZ17, AZ32) to higher (AZ13, AZ16) content of S and Ca. The scatter plot of Ca vs S content, performed selectively on mortars B and C (lime-gypsum mortars) (Fig. 8c) shows that in group B the Ca:S ratio is higher than in group C. Moreover, samples of group B have lower amount of Ca and S, on the whole, in respect to samples of groups C, maybe due to the presence of more aggregate and consequently less binder.

The comparison of compressive strength test results (Table 6) between representative samples of the different groups shows that gypsum mortars of type C exhibit the higher values. The high strength values of sample AZ19 must be related to the high content of halite that in the dry state (crystallized within the mortar mass) acts as a fake cementing material.

3.2. Salt analysis

Most of samples display contamination of soluble salts such as chlorides (halite) and sulphates (gypsum, anhydrite) (Tables 3 and 7). Their presence and their continuous dissolution/crystallization process are associated with the gradual weathering of the mortars.

Sodium chloride or halite (NaCl) is a highly soluble salt with a maximum solubility of 357 g/L at a temperature of 25 °C and equilibrium relative humidity of 75% [40]. In the analyzed samples, smooth rounded surfaces covering the pores and fractures or

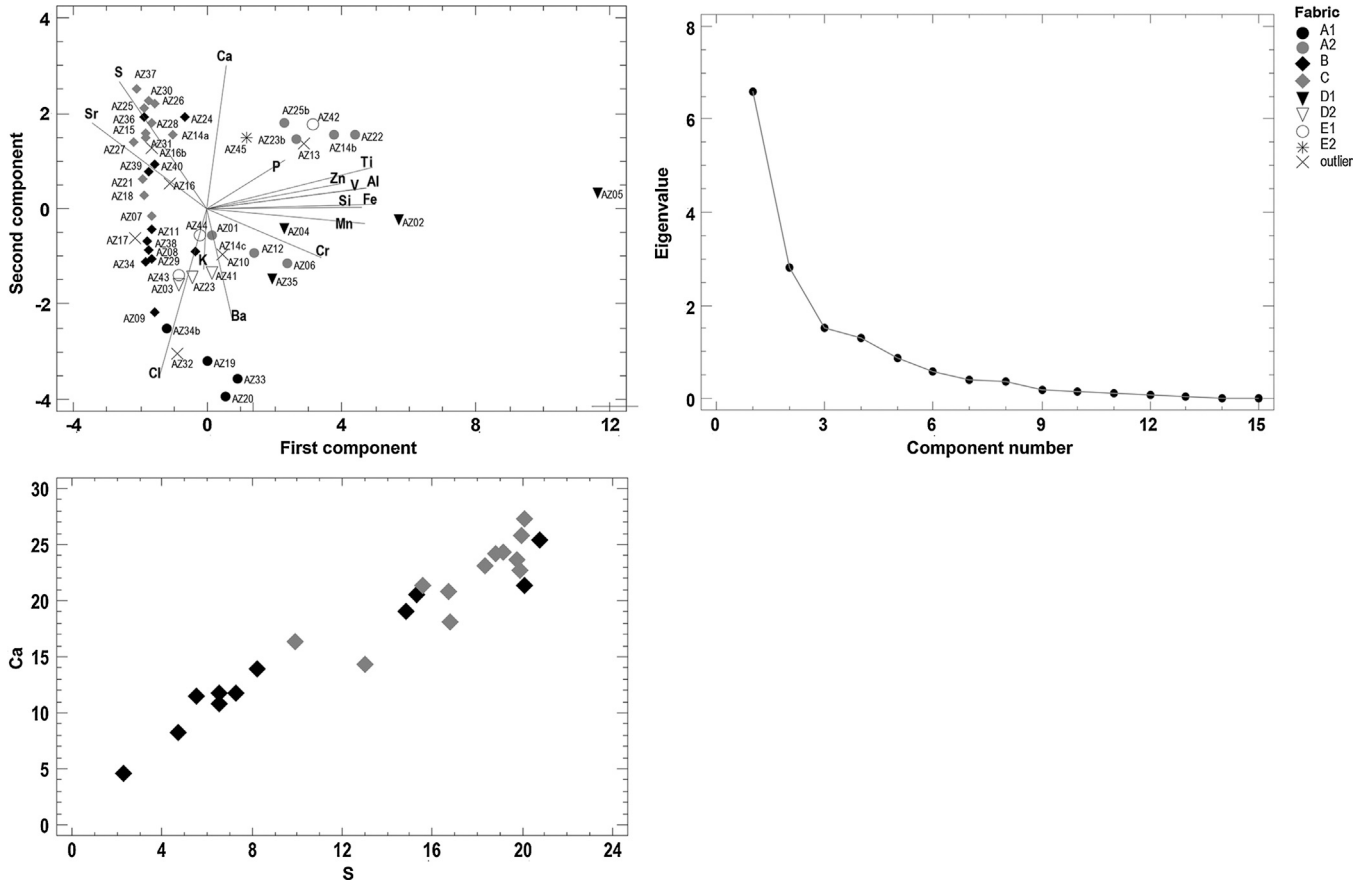

Fig. 8. a–b: principal component analysis of chemical data implemented on the correlation matrix of the elements: a: score and loading plot of principal component 1 vs. principal component 2 explaining 44 and 18% of the total variance, respectively. Together principal components 1 and 2 explain the 62% of the variance of the original data; b: scree plot (eigenvalue profile plot) plotting the eigenvalues attributable to each component; c: scatterplots from Ca vs. S percentage contents, performed selectively on groups B and C.

elongated columnar crystals of NaCl are observed (Fig. 9). Similar morphologies were described and related to moderate to low humidity environments by Theoulakis and Moropoulou [41]. It is likely that similar phenomena control the growth process in Azraq, an environment characterized by very low humidity. At Azraq, the concentration of NaCl depends on the type of mortar rather than the original location of the samples: abundant in groups A1 and, in lower amounts in B, while almost absent in the other types. Therefore, it seems likely that NaCl was originally present in the water added during the slaking process in mortars A1 and B. Very low quantities of NaCl are usually detected in the other samples, probably because of salt spray supply due to the wind action, capillary rise of humidity, or migration from other mortars already enriched with it.

The origin of sulphates must be attributed to the building materials themselves, either to the presence of gypsum mortars or gypsum fragments among the aggregate. Gypsum has very low solubility in dry environments like Azraq; however, the presence of the more hygroscopic sodium chloride (NaCl) lowers its deliquescence humidity with the consequent increase of the solubility [42,43]. In the analyzed samples, recrystallized gypsum inside the pores has columnar, needles like habit or it is in tabular platy crystals (Fig. 9), as typically happens in semiarid environments with low amount of water and humidity [43].

Two samples also show the presence of syngenite (detected by XRD; Table 3): AZ17, as main component, and AZ19 where it is present in small amount. Syngenite ($K_2Ca(SO_4)_2{\cdot}H_2O$) is an uncommon sulphate mineral that has been only rarely found in evaporite deposits, in association with gypsum and halite, but it seems to be unknown in natural deposits in Jordan [44–47]. However, its presence at the Azraq basin cannot be excluded as, in presence of gypsum and potash (K_2O), it can be formed at a temperature of 100 °C, while under hydrothermal condition (high water vapour pressure), this process can happen at 50 °C [39]. Syngenite can also be an intermediate product of the fertilizers production and it is a common constituent of black crusts on buildings where potassium rich, gypsum-bearing building materials are used [39,48,49]. However, the masonries of Azraq castle do not have black crusts. Particularly, sample AZ17 has a light pinkish color (7.5YR 7/3 [50]) and syngenite is the main constituent of the binder (XRD, SEM). At present, the origin of syngenite in these samples cannot yet be attributed and further analyses are required.

4. Discussion

During its long history, the Qasr Azraq has undergone several modifications, which are reflected in different architectural interventions and in the use of diverse mortar typologies, indicative of different traditions.

Mortars of groups B and C were produced by mixing a sulphate binder with lime: group C seems to have undergone an accurate preparation, as suggested by its high homogeneity, very few charcoals, the nearly absence of aggregate, except for gypsum, and the absence of halite; all samples have a light pinkish binder. In contrast, mortars of type B differentiate from group C mostly by their

Table 5
Chemical composition of samples obtained by pXRF; data expressed as wt%.

Sample	Mortar	Ba	Sr	Zn	Fe	Mn	Cr	V	Ti	Ca	K	Al	P	Si	Cl	S
AZ01	A2	0.022	0.021	0.003	0.378	0.022	0.007	**0.001**	0.066	22.774	7.718	**0.001**	0.088	1.255	7.316	1.363
AZ02	D1	0.012	0.015	0.005	2.255	0.030	0.013	0.011	0.273	6.517	6.822	1.643	0.134	8.609	3.417	3.212
AZ03	D2	0.020	0.049	**0.001**	0.390	**0.001**	0.010	**0.001**	0.055	10.238	0.475	**0.001**	**0.001**	2.241	19.700	1.668
AZ04	D1	0.016	0.060	**0.001**	1.301	0.015	0.018	0.013	0.135	13.894	0.687	0.522	**0.001**	4.001	9.631	4.601
AZ05	D1	0.033	0.025	0.009	4.174	0.066	0.023	0.019	0.442	9.723	1.766	2.715	0.208	13.769	0.498	0.348
AZ06	A2	0.034	0.030	0.003	1.803	0.042	0.015	0.006	0.187	18.831	1.486	**0.001**	**0.001**	1.332	15.498	2.546
AZ07	C	0.010	0.111	0.002	0.131	**0.001**	0.009	**0.001**	0.031	16.397	0.483	**0.001**	**0.001**	0.381	16.411	9.887
AZ08	B	0.015	0.136	**0.001**	0.177	**0.001**	0.010	**0.001**	0.034	10.813	2.153	**0.001**	**0.001**	0.821	18.939	6.549
AZ09	B	0.020	0.123	0.002	0.156	**0.001**	0.011	**0.001**	0.022	4.646	10.735	**0.001**	**0.001**	0.373	21.293	2.267
AZ10	Outlier	0.019	0.074	**0.001**	0.710	0.018	0.014	0.007	0.072	14.374	1.004	**0.001**	**0.001**	2.006	13.643	1.739
AZ11	B	0.015	0.122	**0.001**	0.207	**0.001**	0.009	**0.001**	0.040	13.863	5.503	**0.001**	**0.001**	0.724	12.241	8.220
AZ12	A2	0.027	0.022	0.004	0.883	0.028	0.012	0.005	0.132	21.301	1.571	**0.001**	**0.001**	1.195	14.637	0.565
AZ13	Outlier	0.012	0.018	**0.001**	1.961	**0.001**	0.013	0.009	0.289	16.678	0.406	1.195	**0.001**	5.523	0.359	19.019
AZ14a	C	0.017	0.135	**0.001**	0.481	**0.001**	0.007	**0.001**	0.080	21.412	0.594	0.372	0.076	2.014	1.380	15.564
AZ14c	B	0.021	0.117	0.002	0.896	0.012	0.014	**0.001**	0.086	11.742	0.916	**0.001**	**0.001**	1.579	17.409	6.518
AZ14b	A2	0.027	0.048	0.005	1.655	0.026	0.015	0.008	0.314	32.693	1.044	0.540	0.206	2.788	0.501	6.214
AZ15	C	0.016	0.161	**0.001**	0.217	**0.001**	0.009	**0.001**	0.053	23.098	0.458	**0.001**	**0.001**	1.211	3.574	18.365
AZ16	Outlier	0.013	0.093	**0.001**	0.691	0.017	**0.001**	**0.001**	0.096	12.373	12.148	**0.001**	**0.001**	1.938	2.756	20.128
AZ16b	Outlier	0.015	0.162	**0.001**	0.469	**0.001**	0.009	**0.001**	0.070	17.791	2.158	**0.001**	**0.001**	1.426	4.360	19.189
AZ17	Outlier	0.019	0.108	**0.001**	0.325	**0.001**	**0.001**	**0.001**	0.040	7.070	11.017	**0.001**	**0.001**	0.933	13.748	15.948
AZ18	C	0.009	0.132	**0.001**	0.452	**0.001**	0.006	**0.001**	0.049	14.307	0.548	**0.001**	**0.001**	0.489	13.459	12.999
AZ19	A1	0.103	0.022	**0.001**	0.508	0.019	0.008	**0.001**	0.058	9.449	1.135	**0.001**	**0.001**	3.373	21.580	0.671
AZ20	A1	0.151	0.022	**0.001**	0.541	0.016	0.009	**0.001**	0.079	6.201	2.788	**0.001**	**0.001**	5.704	18.965	1.183
AZ21	C	0.015	0.059	**0.001**	0.167	**0.001**	**0.001**	**0.001**	0.036	18.082	0.986	**0.001**	**0.001**	0.892	8.942	16.778
AZ22	A2	0.020	0.025	0.004	1.614	0.042	0.015	0.011	0.338	39.455	0.203	0.480	0.159	2.363	0.194	0.568
AZ23	D2	0.021	0.043	**0.001**	0.459	**0.001**	0.010	0.003	0.073	9.389	1.148	**0.001**	**0.001**	2.478	15.644	1.122
AZ23b	A2	0.012	0.030	0.003	1.340	0.019	0.011	0.008	0.230	33.510	0.310	0.619	0.116	2.577	0.317	3.421
AZ24	B	0.014	0.143	**0.001**	0.690	**0.001**	0.009	0.004	0.100	21.353	0.288	0.352	**0.001**	2.541	0.214	20.070
AZ25	C	0.008	0.124	**0.001**	0.379	**0.001**	**0.001**	**0.001**	0.053	22.697	0.154	**0.001**	0.061	1.561	0.095	19.874
AZ25b	A2	**0.001**	0.037	**0.001**	1.345	0.016	0.014	0.007	0.289	36.385	0.242	0.544	0.112	2.036	0.264	5.312
AZ26	C	0.014	0.133	**0.001**	0.321	**0.001**	**0.001**	**0.001**	0.065	24.358	0.189	0.428	0.068	1.371	0.259	19.153
AZ27	C	0.019	0.148	**0.001**	0.287	**0.001**	**0.001**	**0.001**	0.043	20.867	0.262	**0.001**	**0.001**	0.820	5.886	16.724
AZ28	C	0.014	0.127	**0.001**	0.220	**0.001**	0.008	**0.001**	0.055	23.615	0.191	**0.001**	**0.001**	1.393	0.189	19.774
AZ29	B	0.016	0.114	0.002	0.174	**0.001**	0.008	**0.001**	0.027	11.541	6.337	**0.001**	**0.001**	0.404	17.675	5.536
AZ30	C	**0.001**	0.140	**0.001**	0.264	**0.001**	0.008	**0.001**	0.060	27.348	0.160	**0.001**	**0.001**	1.256	0.142	20.107
AZ31	C	0.013	0.125	**0.001**	0.208	**0.001**	0.008	**0.001**	0.039	24.120	0.127	**0.001**	**0.001**	0.892	4.432	18.791
AZ32	Outlier	0.009	0.016	0.002	0.528	**0.001**	0.012	**0.001**	0.030	1.317	0.089	**0.001**	**0.001**	0.423	34.096	0.682
AZ33	A1	0.075	0.030	**0.001**	1.356	0.018	0.015	**0.001**	0.106	3.644	0.119	0.756	**0.001**	0.983	30.074	0.576
AZ34	B	0.014	0.124	**0.001**	0.172	0.014	**0.001**	**0.001**	0.029	8.292	7.568	**0.001**	**0.001**	0.649	17.691	4.708
AZ34b	A1	0.051	0.025	**0.001**	0.200	**0.001**	0.007	**0.001**	0.030	9.376	6.395	**0.001**	**0.001**	0.728	19.131	0.477
AZ35	D1	0.015	0.018	**0.001**	0.898	0.024	0.008	0.006	0.138	5.437	16.937	0.818	0.172	4.830	6.971	2.597
AZ36	B	0.016	0.142	**0.001**	0.195	**0.001**	0.007	**0.001**	0.048	25.390	0.289	**0.001**	**0.001**	1.137	1.709	20.784
AZ37	C	0.010	0.188	0.002	0.210	**0.001**	**0.001**	**0.001**	0.054	25.810	0.339	**0.001**	0.091	1.259	2.153	19.998
AZ38	B	0.017	0.128	**0.001**	0.161	**0.001**	0.008	**0.001**	0.034	11.731	5.168	**0.001**	**0.001**	0.761	14.657	7.277
AZ39	B	0.011	0.150	0.002	0.141	**0.001**	0.011	**0.001**	0.026	19.104	0.466	**0.001**	**0.001**	0.578	9.556	14.823
AZ40	B	0.014	0.109	0.002	0.158	**0.001**	0.007	**0.001**	0.042	20.492	0.676	**0.001**	0.075	0.816	7.856	15.332
AZ41	D2	0.024	0.045	**0.001**	0.574	0.020	0.010	**0.001**	0.059	14.220	0.892	0.640	**0.001**	1.786	17.443	1.262
AZ42	E1	0.023	0.035	0.006	0.539	0.042	**0.001**	**0.001**	0.133	27.384	1.956	0.628	0.982	4.933	1.846	1.361
AZ43	E1	0.016	0.028	0.003	0.203	**0.001**	0.009	**0.001**	0.039	16.306	1.252	**0.001**	**0.001**	0.462	21.183	1.394
AZ44	E1	0.023	0.024	0.004	0.267	0.013	0.008	**0.001**	0.049	22.724	2.361	**0.001**	**0.001**	0.789	11.757	2.878
AZ45	E2	0.020	0.012	0.007	0.437	0.016	**0.001**	**0.001**	0.087	39.736	0.467	0.541	0.045	2.419	0.583	0.533
Mean		0.023	0.081	0.002	0.672	0.011	0.009	0.003	0.098	17.644	2.533	0.252	0.052	2.095	9.849	8.641
StDev		0.025	0.053	0.002	0.733	0.014	0.005	0.004	0.095	9.172	3.720	0.501	0.145	2.331	8.681	7.749

The value 0.001 is given in case of non-detected elements due to very low concentration (bold). Mean and standard deviations (StDev) are calculated, too.

heterogeneous, highly porous, grey binders, with different proportions of sulphates and lime (with lime usually exceeding the sulphates content). Charcoals, probably residue of the firing process, are often present [37,38,51], and halite is always present in small amounts. According to these differences, mortars of group B seem to be produced following faster and less standardized methods. The cause of the different binder colors (greyish and pinkish) between these two types is probably due to the difference in the Ca/S ratio (higher in B), and in the presence in mortar B of rock types among the aggregate and more abundant charcoals that can act as pigment darkening the color [37,52,53]. The choice of mixing a sulphate binder with lime suggests a good knowledge of mortar technology since it has fast initial setting, due to the presence of calcium sulphate hemihydrate ($CaSO_4 \cdot 1/2H_2O$), while the lime guarantees good mechanical properties and water resistance [54].

Table 6
Compressive strength test data.

Sample	Mortar	Compressive strenght (MPa)
AZ19	A1	10.92
AZ12	A2	1.88
AZ36	B	3.29
AZ27	C	6.58
AZ31	C	5.26
AZ04	D1	1.73
AZ10	Outlier	3.68

Besides gypsum mortars, lime-based mortars (A1, A2, E1, E2) were used: mortar A1 is characterized by evident fissuring developed during the shrinkage of the binder [37,38], and a poorly sorted angular aggregate, suggesting intentional grinding. The very high amount of halite may suggest that it was originally present in

Table 7
Quasi-quantitative concentration of soluble salt ions carried out through colorimetric test strips; 2 g of each sample was dissolved in 100 mL of distilled water.

Sample	Height (cm)	Mortar group	Sulphates (SO_4^-)	Chlorides (Cl^-)	Nitrates	
					NO_2^-	NO_3^-
			mg/L			
AZ110	290	A2	>1600	500	500	250
AZ111	10	A2	>1600	500	250	250
AZ112	160	A2	>1600	500	250	
AZ113	290	B	>1600	500	500	250
AZ114	160	B	>1600	500	250	
AZ115	10	B	>1600	500	250	
AZ116	290	A1	>1600	≥3000	500	
AZ117	10	A1	>1600	1000	250	
AZ118	160	A1	>1600	≥3000	500	
AZ120	290	C	>1600	500	250	
AZ121	160	C	>1600	500	250	500
AZ122	10	C	>1600	500	250	

the water added during the slaking process [51]. However, mortar group A1 is not very homogeneous and its components may also be referred to different construction phases of the site. Lime mortar A2 differs from A1 mainly in the aggregate rock types, which is well sorted and rounded, suggesting that it derives from a loose sediment, collected and sieved. Mortar E1 has a compact binder and almost no aggregate. Type E2 is the only hydraulic mortar found at Azraq, the aggregate is almost exclusively represented by angular fragments of partially burned limestone. A few samples of groups A2 and E1 are feebly hydraulic, probably as a reaction to the presence of volcanic rocks among the aggregate or clayey impurities in the original carbonatic rocks that can cause a limited hydraulicity if fired at temperatures between 600–900 °C [37,51]. It is possible that feeble lime-pozzolan reactions have not been detected by XRD in most of the samples because the new hydrate phases are present in small quantities, and their microstructure may have not been stable and partially destroyed by the fast carbonation, due to the warm environment [55,56]. It is not clear whether volcanic rock fragments were added with the aim to provide hydraulicity to the mortars or because they were abundant in the sediments near the site.

Earthen mortars (D) were used, too; they are often made by terrigenous materials mixed with lime to obtain a better performance and increase their strength. Among the aggregate, there are also unburned vegetable fibres, indicating that they did not undergo a firing process.

Dolomitic plaster was identified only in one room (AZ10). Dolomite may be a residue of the starting raw material, probably due to incomplete dissociation at temperatures lower than 750 °C [57,58]. Minerals product of the carbonation process, such as brucite and portlandite, are absent [57].

Finally, only sample AZ17 is mainly composed of syngenite and gypsum. These last two mortar types (AZ10, AZ17) are outliers and cannot be considered for a general reconstruction of the building techniques applied at Azraq.

The presence in the region of lime mortar with pozzolanic aggregate (mortars A1, A2, E1, E2) has Roman origin but it was reproduced in later periods, too, as in the near Umayyad mosques at Hallabat, and in different buildings at Amman Citadel [59]. The technique of gypsum-lime mortars (types B, C) finds its origin in the Sassanian tradition (224–651 AD). Sassanians invaded Jordan between 610–629 AD, and this technique was used in the near Umayyad sites of Qusayr Amra and Qasr Harane [60]; however, probably due to the proximity of the Sassanian empire, gypsum-lime mortar was already known in Jordan before their occupation, as found at the Roman site of Jerash [61].

In some cases, it was possible to define a relative chronology of the mortars, thanks to superimpositions of different mortar types: mortar A2 can probably be traced to the Ayyubid period, since it is present on the structures involved in the Ayyubid reconstruction dated 1237 AD, and appears to be the most recent of the studied mortars. It was used with pointing and plaster/rendering functions, and it covers mortars of type B and C (cf. AZ25, AZ25b; AZ14, AZ14c, AZ14b; Fig. 4a). On the external wall, it was also used as a render to protect the wall and it covers the pointing lime-earthen mortar D2 (samples AZ23b, AZ23), suggesting that D2 was coeval or older. Gypsum-lime mortar B appears to be more recent than lime mortar A1 (cf. AZ34, AZ34b; Fig. 4a) and C (cf. AZ14, AZ14c; Fig. 4a) and it may be referred to remedial interventions as it seems produced following fast and non-standardized processes. Finally, there are no direct connections between mortars A1 and types A2, and C. Mortars from the mosque (E1, E2) do not have any relation with the other types present at the site.

5. Conclusions

The multi-analytical approach adopted in this research allowed to group and characterise the mortars used at Qasr Azraq (Jordan) and to achieve a better understanding of the building materials and techniques employed at the site during its lifetime.

The most important events involving the castle seem to be its foundation dated to Diocletian and Maximilian time (287–305 AD) or earlier, a refurbishment under Constantine (326–333 AD) and an important reconstruction under the Ayyubids, dated 1237 AD. During Ayyubid time, the castle was partially re-plastered with a lime mortar mixed with well-sorted and round aggregate of igneous volcanic origin (A2). It was not possible to precisely date the use of other mortar types; however, hydraulic lime mortar with pozzolanic aggregate has Roman origin, while gypsum-lime mortar derives from the Sassanian tradition and it seems possible that it was not highly used in Jordan when the castle was built. The data suggest that lime mortar (A1), prepared with a poorly sorted angular volcanic aggregate, is the oldest used at the site; this would explain why we have only a few samples, generally poorly preserved. Therefore, the pinkish gypsum-lime mortar (C) may be referred to a more recent event, perhaps the refurbishment made under Constantine. The grey lime-gypsum mortar (B) seems to be referred to successive remedial interventions. However, these are speculations, and a more accurate stratigraphic study must be done. The mortars in the mosque (E1, E2) are different from all the other studied at the site; therefore it seems likely that the mosque construction is not coeval with the main building phases.

Acknowledgments

The authors would like to thank the Department of Antiquities of Jordan for providing samples, particularly Mr. Ahmad Lash and Wesam Esaid. We would like to thank also Lorraine Abu-Azizeh, Qutaiba Dasouqi and Yahya Alshawabkeh for helping with the photogrammetry, and the personnel at the Institute of Nanoscience and Nanotechnology, NCSR Demokritos where the analyses were carried out.

The research was conducted within the framework of the New Archaeological Research Network for Integrating Approaches to ancient material studies (NARNIA) Project, a Marie Curie

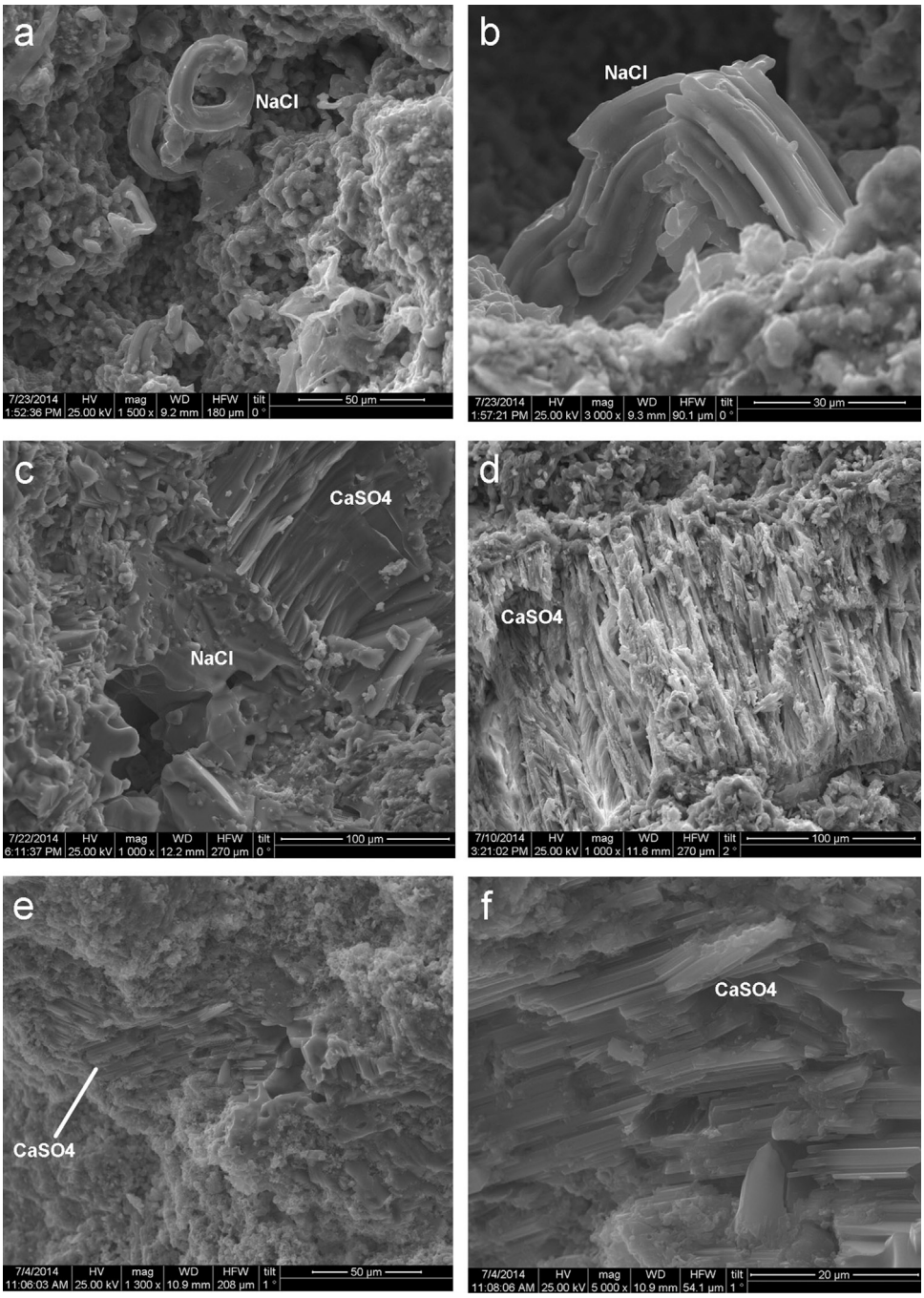

Fig. 9. BSE–SEM images showing different microtextures of re-crystallized soluble salts present in the studied mortars: a–b: sample AZ39; c: sample AZ34a; d: sample AZ14; e–f: sample AZ23b.

Initial Training Network funded by the FP7 and the European Union.

Appendix A. Supplementary data

Supplementary data associated with this article can be found, in the online version, at https://doi.org/10.1016/j.culher.2018.03.005.

References

[1] D. Kennedy, Archaeological explorations on the Roman frontier in north-east Jordan, in: BAR international series 134, Archaeopress, Oxford, 1982.
[2] A. Lash, Restoration and excavation at al-Azraq castle during 2008, in: Annual of the Department of Antiquities, 2009, pp. 423–431.
[3] D. Kennedy, The Roman army in Jordan, in: Council for British Research in the Levant, Oxbow Books, Oxford, 2004.
[4] D. Kennedy, D. Riley, Rome's desert frontier from the air, Batsford, London, 1990.
[5] P. Freeman, The Roman period, in: R.B. Adams (Ed.), Jordan: an archaeological reader, Equinox, London, 2008, pp. 413–441.
[6] S. Gregory, D. Kennedy, Sir Aurel Stein's limes report, in: BAR International series 272, Archaeopress, Oxford, 1985.
[7] D. Kennedy, H.I. McAdam, Some Latin inscriptions from the Azraq oasis, Jordan, Zeitschrift für Papyrologie und Epigraphik 60 (1985) 97–107.
[8] S.T. Parker, Roman and Saracens: a history of the Arabian frontier, Eisenbrauns, Winona Lake IN, 1986.
[9] I. Arce, Coenobium, palatium and hira: the Ghassanid complex et al-Hallabat. Studies in the history and archaeology of Jordan, in: F. Al-Khraysheh (Ed.), Proceedings of the 10th international conference ICHAJ (Washington May 2007), Amman, 2009, pp. 937–966.
[10] I. Arce, Romans, Ghassanids and Umayyads and the transformation of the limes Arabicus: from coercive and deterrent diplomacy towards religious proselytism

and political clientelarism, in: G. Vannini, M. Nucciotti (Eds.), La Transgiordania nei secoli XII-XIII e le "frontiere" del Mediterraneo medievale, BAR international series 2386, Archaeopress, Oxford, 2012, pp. 55–74.
[11] D.F. Graf, The Saracens and the defence of the Arabian frontier, Bull. Am. Sch. Orient. Res. 229 (1978) 1–26.
[12] P. Watson, The Byzantine period, in: R.B. Adams (Ed.), Jordan: an archaeological reader, Equinox, London, 2008, pp. 495–537.
[13] Tabari (738–745), Ta−ri−kh al-rusul wa-al-mulu−k (The History of al-Tabari Vol. 26. The waning of the Umayyad caliphate: prelude to revolution), State University of New York Press, Albany NY, 1989 (C. Hillenbrand, translator).
[14] A. Walmsley, Fatimid, Ayyubid and Mamluk Jordan and the crusader interlude, in: B. McDonald, R. Adams, P. Bienkowski (Eds.), The archaeology of Jordan, Sheffield Academic Press, Sheffield, 2001, pp. 515–559.
[15] A. Walmsley, The Middle Islamic and crusader period, in: R. Adams (Ed.), Jordan, an archaeological reader, Equinox, London, 2008, pp. 495–537.
[16] A. Damick, A. Lash, The past performative: thinking through the Azraq community archaeology project, Near Eastern Archaeology 76 (3) (2013) 142–150.
[17] R. Bocco, The settlement of pastoral nomads in the Arab Middle East: international organizations and trends in development policies 1950-1990, in: D. Chatty (Ed.), Nomadic societies in the Middle East and North Africa: entering the 21st century, Brill, Leiden, 2006, pp. 302–334.
[18] S. Gregory, Roman military architecture on the eastern frontier, Adolf M. Hakkert, Amsterdam, 1995.
[19] S. Gregory, Was there an eastern origin for the design of late Roman fortification? Some problems for research on forts of Rome's eastern frontier, in: D. Kennedy (Ed.), The Roman army in the East, Journal of Roman archaeology supplementary series No. 18, JRA, 1996, pp. 169–209.
[20] I. Arce, From the diaphragm arches to the ribbed vaults. A hypothesis for the birth and development of a building technique, in: S. Huerta (Ed.), Proceedings of the first international congress on construction history (Madrid, 20th–24th January 2003), Madrid, 2003, pp. 225–241.
[21] W. Bajjali, K. Khair Al-Hadidi, Hydrochemical evaluation of groundwater in Azraq Basin (Jordan) using environmental isotopes and GIS techniques, in: 25th annual ESRI international user conference (San Diego, California, July 25–29, 2005), ESRI International, Redlands, CA, 2005.
[22] F. Bender, Geology of the Arabian Peninsula, Jordan, Geological survey professional paper 560-I, U.S. Government Printing Office, Washington, 1975.
[23] A.N. Garrad, B. Byrd, P. Harvey, F. Hivernel, Prehistoric environment and settlement in the Azraq basin: a report on the 1982 survey season, Levant 17 (1985) 1–28.
[24] H. Alfugha, The nature of Pleistocene volcanism in the north-eastern Jordan, in: The geological society of America 125th anniversary annual meeting (27–30 October Denver, Colorado), 2013 (URL: https://gsa.confex.com/gsa/2013AM/webprogram/Paper220213.html).
[25] F.M. Howari, K.M. Banat, Y.A. Abu-Salha, Depositional and diagenetic processes of Qa Khanna playa, north Jordan basaltic plateau, J. Asian Earth Sci. 39 (4) (2010) 275–284.
[26] European Standard EN 12407: 2000 Natural stone test methods - Petrographic examination, Brussels: European Committee for Standardization.
[27] Norma Italiana UNI 11176: 2006 Beni Culturali – Descrizione petrografica di una malta ICS: [91.100.10]. Cultural heritage – petrographic description of a mortar.
[28] H. Alison, J. Stewart (Eds.), Mortars, renders & plasters – practical building conservation, Routledge, London, 2012.
[29] J. Lanas, R. Sirera, J.I. Alvarez, Compositional changes in lime-based mortars exposed to different environments, Thermochimica Acta 429 (2) (2005) 219–226.
[30] J.M. Valverde, S. Medina, Crystallographic transformation of limestone during calcination under CO_2, Phys. Chem. Chem. Phys. 17 (34) (2015) 21912–21926.
[31] M. Drdácký, Non-standard testing of mechanical characteristics of historic mortars, Int. J. Architect. Herit. 5 (4–5) (2011) 383–394.
[32] J. Válek, R. Veiga, Characterisation of mechanical properties of historic mortars–testing of irregular samples, in: C.A. Brebbia (Ed.), Structural studies, repairs and maintenance of heritage architecture IX, WIT Transactions on the built environment 83, WIT Press, 2005, pp. 365–374.
[33] M. Drdàcký, D. Makšìn, M.D. Mekonone, Z. Slìžkovà, Compression tests on non-standard historic mortar specimens, in: Proceedings of HMC 2008 "Historic mortar conference", Lisbon, 2008 (URL: https://web.natur.cuni.cz/uhigug/masin/download/DMMS_HMC08.pdf).
[34] R.S. Boynton, Chemistry and technology of lime and limestone, Wiley, New York, 1980.
[35] J. Elsen, K. Van Balen, G. Mertens, Hydraulicity in historic lime mortars: a review, in: J. Válek, C. Groot, J.J. Hughes (Eds.), Proceedings of HMC2010 "Historic Mortars Conference", Springer, Netherlands, 2010, pp. 129–145.
[36] K. Callebaut, J. Elsen, K. Van Balen, W. Viaene, Nineteenth century hydraulic restoration mortars in the Saint Michael's Church (Leuven, Belgium). Natural hydraulic or cement? Cem. Concr. Res. 31 (2001) 397–403.
[37] J. Elsen, Microscopy of historic mortars – a review, Cem. Concr. Res. 36 (2006) 1416–1424.
[38] E. Pecchioni, F. Fratini, E. Cantisani, Atlante delle malte antiche in sezione sottile al microscopio ottico – Atlas of the ancient mortars in thin section under optical microscope, Nardini editore, 2014.
[39] J.T. Kloprogge, L. Hickey, L.V. Duong, W.N. Martens, R.L. Frost, Synthesis and characterization of $K_2Ca_5(SO_4)_6{\cdot}H_2O$, the equivalent of görgeyite, a rare evaporite mineral, Am. Mineral. 89 (2004) 266–272.
[40] P. Brimblecombe, C.M. Grossi, Damage to buildings from future climate and pollution, APT Bull. 38 (2–3) (2007) 13–18.
[41] P. Theoulakis, A. Moropoulou, Salt crystal growth as weathering mechanism of porous stone on historic masonry, J. Porous Mater. 6 (1999) 345–358.
[42] E. Borrelli, A. Urland, ARC Laboratory handbook: conservation of architectural heritage, historic structures and materials, ICCROM, 1999 (URL: http://www.iccrom.org/pdf/ICCROM_14_ARCLabHandbook00_en.pdf).
[43] A.E. Charola, J. Puhringer, M. Steiger, Gypsum: a review of its role in the deterioration of building materials, Environ. Geol. 52 (2) (2007) 339–352.
[44] J.W. Anthony, R.A. Bideaux, K.W. Bladh, M.C. Nichols, Handbook of Mineralogy 5, Mineral Data Publishing, Tucson, Arizona, 1990–2003 (URL: http://www.handbookofmineralogy.org/pdfs/syngenite.pdf).
[45] W.A. Deer, R.A. Howie, J. Zussman, Rock forming minerals, Vol. 5: non-silicates: sulphates, carbonates, phosphates and halides, Geol. Soc. 5 (1996).
[46] L.I. Gorogotskaya, N.V. Podberezskaya, S.V. Borisov, Refinement of the crystal structure of syngenite $K_2Ca(SO_4)_2{\cdot}H_2O$, J. Struct. Chem. 9 (1) (1968) 69–72.
[47] Mindat: public database of mineral information. URL: http://www.mindat.org/min-3856.html.
[48] V. Matović, S. Erić, A. Kremenović, P. Colomban, D. Srećković-Batoćanin, N. Matović, The origin of syngenite in black crusts on the limestone monument King's Gate (Belgrade Fortress, Serbia) – the role of agriculture fertiliser, J. Cult. Herit. 13 (2) (2012) 175–186.
[49] K. Wieczorek-Ciurowa, Topochemistry of thermal dehydration of syngenite $K_2Ca(SO_4)_2{\cdot}H_2O$, Thermochimica Acta 92 (1985) 485–487.
[50] A. Munsell, Munsell soil color chart, Kollmorgen Instruments Corporation, Macbetch Division, New York, 1994.
[51] E. Pecchioni, F. Fratini, E. Cantisani, Le malte antiche e moderne tra tradizione ed innovazione, Patron Editore, Bologna, 2008.
[52] C. Rodriguez-Navarro, Binders in historical buildings: traditional lime in conservation, in: J.M. Herrero, M. Vendrell (Eds.), International seminar on archaeometry and cultural heritage: the contribution of mineralogy (Bilbao 27th June 2012), SEM 09, 2004, pp. 92–111.
[53] R.F. Rubio-Domene, El material de yeso: comportamiento y conservación, Cuadernos Restauracion 6 (2006) 57–68.
[54] G. Torraca, Lectures on materials science for architectural conservation, Getty Conservation Institute, LA, USA, 2009 (URL: http://www.getty.edu/conservation/publications_resources/pdf_publications).
[55] G. Cultrone, E. Sebastián, M. Ortega Huertas, Forced and natural carbonation of lime-based mortars with and without additives: mineralogical and textural changes, Cem. Concr. Res. 35 (2005) 2278–2289.
[56] M. Radonjic, K.R. Hallam, G.C. Allen, R. Hayward, Mechanism of carbonation in lime-based materials, in: Proceedings of the 8th Euro-seminar on microscopy applied to building materials, Athens (Greece), 2001, pp. 465–475.
[57] H. Hartshorn, Dolomitic lime mortars: carbonation complications and susceptibility to acidic sulphates (Master's Thesis), Columbia University Historic Preservation, 2012.
[58] M.V. Belousov, E.N. Selivanov, R.I. Gulyaeva, S.N. Tyushnyakov, D.F. Rakipov, Thermodynamics and kinetics of thermal dissociation of dolomite, Russ. J. Non Ferrous Met. 57 (3) (2016) 180–186.
[59] I. Arce, Early Islamic lime kilns from the Near East. The cases from Amman Citadel, in: S. Huerta (Ed.), Proceedings of the first international congress on construction history (Madrid, 20–24th January 2003), Madrid, 2003, pp. 213–224.
[60] I. Arce, Umayyad building techniques and the merging of Roman-Byzantine and Partho-Sassanian traditions: continuity and change, in: L. Lavan, E. Zanini and A. Sarantis (Eds.), Late antique archaeology: technology in transition A.D. 300–650, 4, 2008, pp. 491–537.
[61] I.A. Bani Yaseen, H. Al-Amoush, M. Al-Farajat, A. Mayyas, Petrography and mineralogy of Roman mortars from buildings of the ancient city of Jerash, Jordan, Constr. Build. Mater. 38 (2013) 465–471.
[62] APAAME: Aerial photographic archive for archaeology in the Middle East. URL: http://www.apaame.org/.
[63] J.M. Teutonico, A laboratory manual for architectural conservators, ICCROM, Rome, 1988, pp. 52–55 (URL: http://www.iccrom.org/sites/default/files/ICCROM_11_LabManual_en.pdf).